RSC Advances

PAPER

View Article Online
View Journal | View Issue

Cite this: *RSC Adv.*, 2023, **13**, 11685

Synthesis, characterization and properties of a novel environmentally friendly ternary hydrophilic copolymer

Wentao Ma,[a] Lu Yang,[b] Yang Wu,[c] Yu Zhang,*[a] Cong Liu,[b] Jie Ma[a] and Bingqi Sun[a]

A novel environmentally friendly scale inhibitor was synthesized by the free radical polymerization of itaconic acid (IA), acrylamide (AM), and sodium *p*-styrene sulfonate (SSS). The structures of the copolymers were characterized using FTIR, UV, and ^{1}H-NMR, which proved successful in obtaining the expected target structures. The synthesis conditions such as monomer ratio, initiator dosage, titration time, and reaction temperature were optimized by the static scale inhibition method, and the expected polymeric scale inhibitor with a competent scale inhibition performance was obtained. The copolymer conversions at different temperatures were obtained indirectly by bromination titration, and the relationship between the molecular weight of the polymer and the scale inhibition performance at different reaction temperatures was also investigated by GPC. The results showed that the copolymer had a good ability to control calcium carbonate scaling, and the inhibition rate of $CaCO_3$ reached 84.7% at a dose of 30 mg L^{-1}. The microscopic morphology and structure of calcium scales were analyzed by SEM, FTIR, and XRD, and it was concluded that the copolymer could change the crystallization path of calcium carbonate from stable calcite to vaterite. That could be dispersed in water. The proposed inhibition mechanism suggests that surface complexation between polymer functional groups and Ca^{2+} leads to excellent solubility of the complexes. These findings suggest that the prepared green copolymers have great potential for oilfield applications.

Received 7th February 2023
Accepted 27th March 2023

DOI: 10.1039/d3ra00811h

rsc.li/rsc-advances

1. Introduction

Water injection is an important measure to replenish the energy of oil reservoirs and to improve recovery during oil extraction. To improve the recycling rate of water, the recovered water is usually treated and reinjected. Oilfield wastewater is a complex multiphase system containing solids–liquid, impurities, gases, and dissolved salts.[1,2] when more than two types of unmatched water in the fluid are mixed or the chemical components of the fluid are imbalanced during the flow process caused by changes in pressure and temperature, it easily leads to the scaling phenomenon. $CaCO_3$ scale is one of the most common scales in oil and gas production systems, and calcium scale is usually found in underground equipment, pipelines, valves, wellheads, and other places.[3,4] Scaling can easily damage oil production equipment and transmission pipelines, which seriously affects the normal production of oil and gas fields.[5] Especially in low permeability fields, scaling can block reservoir pores, causing reservoir permeability to decrease and injection pressure to increase, resulting in under-injection of injection wells, which leads to a decrease in oil production.[6]

Water-soluble polymeric materials have been applied in the prevention and control of oilfield fouling, and polymers with multiple functional groups have been shown to play a key role in the inhibition of fouling in water treatment.[7] Therefore, the development and performance testing of polymers has become important topics in the field of water treatment today. Cui *et al.* developed a water-soluble green polymer based on itaconic acid (IA) and 2-acrylamido-2-methylpropanesulfonic acid (AMPS), which exhibited excellent scale inhibition performance against calcium carbonate;[8] Li *et al.* synthesized an environmentally friendly terpolymer PAA-AEO-SAS using acrylic acid (AA), fatty alcohol polyoxyethylene ether (AEO) and sodium allyl sulfonate (SAS) as raw materials. The combination of multiple functional groups allows PAA-AEO-SAS to be applied in complex water environments.[9] In addition, because of the expensive cost of green scale inhibitors and other reasons, researchers have made many efforts on their modifier. For example, a new scale inhibitor poly aspartic acid derivative (PASP-Im) was synthesized by Guo *et al.* using poly succinimide and iminodiacetic acid as raw materials. With the introduction of the

[a]*College of Chemistry and Environmental Engineering, Hubei Minzu University, Enshi 445000, Hubei, People's Republic of China. E-mail: zy_9915@163.com*
[b]*No. 3 Oil Production Plant of PetroChina Changqing Oilfield Company, Yinchuan, 750005, Ningxia, People's Republic of China*
[c]*Xi'an 3D Technology Development Co., Xian 710016, Shanxi, People's Republic of China*

iminodiacetic acid group, the synthesized PASP-Im exhibited better scale inhibition performance against $CaCO_3$ deposits than the unmodified PASP.[10] Shi *et al.* synthesized a new scale and corrosion inhibitor poly aspartic acid/furfuryl amine graft copolymer (PASP/FA) using maleic anhydride, urea, and furfuryl amine (FA) as raw materials. Compared with PASP, its overall performance was significantly improved.[11] It is not difficult to find that the research on scale inhibitors is mainly focused on green polyfunctionalization and modification.

The inhibitory properties of polymer inhibitors are highly dependent on their polymer structure, molecular weight, and functional groups.[12] Common functional groups are carboxylic acid groups, sulfonic acid groups, and hydroxyl groups.[13] Based on the complex water environment in the oilfield, multifunctional polymeric scale inhibitors are usually used. The hydrophilic carboxyl group is the main functional group to inhibit calcium carbonate, but its low dispersion hinders the efficiency of scale inhibition.[14] To compensate for the lack of scale inhibition performance of carboxyl groups, sulfonic acid groups and amide groups are considered. The sulfonic acid group is a strong hydrophilic group, which not only increases the water solubility but also prevents the formation of calcium gel.[12,15] The amide group increases the solubility of the inhibitor by forming hydrogen bonds and reacts with calcium ions to enhance the adsorption ability of the inhibitor on the particle surface.[16] In addition, the heteroatoms in these groups of polymeric scale inhibitors, such as O, N, and S, have high electron density and can form multiple bonds, which can provide multiple adsorption sites and promote the ability to chelate metal cations to make them adsorbed on the crystal surface of the sediment.[17–19]

In this research work, sulfonic acid groups and amide groups were introduced into the molecular structure of IA copolymers by free radical polymerization. The phosphorus-free multi-hydrophilic group copolymer IA-AM-SSS scale inhibitor containing carboxyl, sulfonic acid, and amide groups was prepared by using IA, AM, and SSS as monomers, water as a solvent and ammonium persulfate as an initiator. The effects of monomer ratio, initiator dosage and titration time, and reaction temperature on the performance of copolymers were investigated by single-factor tests. The structure of IA-AM-SSS was verified by FTIR, UV, and ^{1}H-NMR. Scaling efficiency against $CaCO_3$ was tested using a static experimental method. The conversion rate of the copolymer was indirectly obtained by bromine titration, and the molecular weight of the copolymer was determined by GPC. Thermogravimetric analysis was performed to investigate the thermal stability of the copolymers. The morphological and structural characteristics of the crystals were obtained using SEM, FT-IR, and XRD, and the mechanism of scale inhibition of IA-AM-SSS was discussed in detail based on the conclusions of the crystallographic analysis.

Notably, an IA/AM/SSS adaptive retarder was synthesized by Zhang *et al.* In the performance evaluation of cement slurries (or cured cement), acceptable thickening times and adequate early compressive strengths were obtained, and the "super-lag" phenomenon of cement slurries was avoided at relatively low temperatures and pressures. This improves the adaptability of the cement slurry to further meet the engineering requirements of drilling operations. Therefore, IA-AM-SSS polymer has great potential for oilfield applications.[20]

2. Experimental section

2.1 Materials

IA (itaconic acid) and SSS (sodium p-styrene sulfonate) used in the experiments were purchased from Shandong Usolf Chemical Technology Co., Ltd. in China, AM was supplied by Shanghai Aladdin Biochemical Technology Co., Ltd. in China, and ammonium persulfate ($(NH_4)_2S_2O_8$) was purchased from Shanghai Macklin Biotechnology Co. Other anhydrous calcium chlorides, sodium bicarbonate, potassium hydroxide, potassium chloride, sodium tetraborate decahydrate, disodium EDTA and calcium carboxylate were purchased from Sinopharm (Shanghai, China) Chemical Reagent Co., IA, and SSS were of technical grade, all other chemicals were of analytical reagent grade, all solutions were prepared using deionized water.

2.2 Synthesis of IA-AM-SSS

IA-AM-SSS was synthesized in a three-necked round bottom flask equipped with a thermometer, magnetic stirrer, and reflux unit under a nitrogen atmosphere. The copolymer was synthesized by free radical polymerization in an aqueous medium using ammonium persulfate as an initiator, and SSS and an appropriate amount of deionized water was first added in a predesigned ratio, heated to 50 °C, and dissolved. After that, IA was added to the above solution, and after IA was completely dissolved under continuous stirring conditions, AM dissolved in deionized water was added to the flask. Then the temperature was raised rapidly to 80 °C and kept at this temperature, and ammonium persulfate aqueous solution was added dropwise at a constant flow rate (dropping for 2 h). After that, the reaction temperature was raised to 85 °C and the reaction was continued for 1 h. When the reaction was finished, the prepared yellow copolymer was obtained. After cooling and weighing, the unreacted monomer was removed by a dialysis membrane and freeze-dried for 48 h to obtain the purified polymer product. The synthesis scheme for the copolymer is shown in Fig. 1.

2.3 Measurements and characterization

2.3.1 FTIR and UV. The success of the reaction was first verified using an FT-IR and UV analyzer, which meant that the product met our expectations. FTIR spectra were recorded on a Nicolet AVATAR 360FT-IR spectrometer (Nicolet, American) using KBr pellets between 4000 and 500 cm^{-1}, and UV spectra were recorded on a METASH UV-8000S spectrophotometer (Shanghai, China) equipped with a dual-beam optical system.

2.3.2 ^{1}H NMR. Hydrogen nuclear magnetic resonance spectroscopy (^{1}H NMR, Bruker Advance III 400 MHz, Germany) of the copolymer was obtained by a nuclear magnetic resonance spectrometer with D_2O as the solvent. To further validate the functional groups of the synthesized polymers, which play an important role in the anti-scaling properties. After the analysis of the FT-IR, UV, and ^{1}H NMR spectra, it's known that the expected product was synthesized successfully.

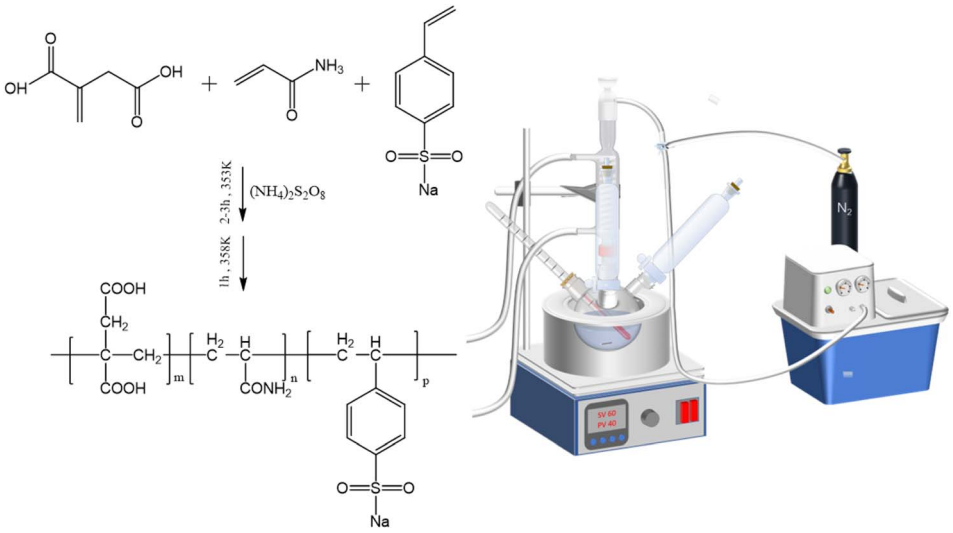

Fig. 1 Experimental setup and IA-AM-SSS synthesis route.

2.3.3 TGA. The thermal properties of the copolymer were obtained by Thermogravimetric Differential Thermal Synchronous Heat Analyzer (SEIKO TG/DTA 6300, Japan) in a temperature range of 30 °C to 800 °C at a heating rate of 10 °C min^{-1} in nitrogen.

2.3.4 GPC. The weight distribution of the polymer was determined by gel permeation chromatography (GPC, TRSEC MODEL302) with water as the mobile phase at a flow rate of 1.0 mL min^{-1} calibrated with PEG standards.

2.3.5 SEM and XRD. The morphology and crystal size of the calcium carbonate scale were observed by scanning electron microscopy (SEM, TESCAN MIRA LMS). The crystal structure was observed by X-ray powder diffraction (SHIMADZO XRD-7000, Japan) with a Cu-Kα radiation source (40 kV and 30 mA).

2.4 Evaluation of antiscalant behavior (static bottle test method)

The anti-$CaCO_3$ performance of the copolymer was determined by the static scale inhibition method according to Chinese standard GB 16632-2019 (China) Determination of scale inhibition performance of water treatment agents by calcium carbonate deposition method.

The experimental procedure was as follows: $CaCl_2$ and $NaHCO_3$ were used to prepare saturated solutions with Ca^{2+} and HCO_3^- concentrations of 6 mg mL^{-1} and 18.3 mg mL^{-1}. Add a certain amount of copolymer solution to the resulting solution, $Na_2B_4O_7$ solution is used to adjust the pH of the test solution to 9.0, in addition to adding the copolymer scale inhibitor, prepare a blank solution without copolymer scale inhibitor at the same time, keep the prepared solution at a constant temperature of 80 °C for 10 hours, filter it while it is hot with neutral filter paper, and titrate the Ca^{2+} concentration in the filtered solution with EDTA standard solution after cooling to room temperature.

The scale inhibition performance η is calculated by the formula (1) with the value expressed as 100%:

$$\eta = \frac{\rho_4 - \rho_3}{\rho - \rho_3} \times 100\% \quad (1)$$

where: ρ_4 – the value of calcium ion (Ca^{2+}) mass concentration after adding the test solution of water treatment agent; ρ_3 – the value of calcium ion (Ca^{2+}) mass concentration after the test solution of blank test solution without water treatment agent; ρ – the value of calcium ion (Ca^{2+}) mass concentration in the prepared water.

2.5 Conversion rate measurement

The extent of the polymerization reaction can be expressed in terms of the monomer conversion rate, which can generally be measured in terms of the double bond content of the reaction product. The residual content of the itaconic acid monomer (bromine value) is the number of double bonds in the polymer that can be added by bromine, which can indirectly reflect the degree of the polymerization reaction. The higher the bromine value, the higher the double bond content and the lower the monomer polymerization conversion; on the contrary, the higher the monomer polymerization conversion. The experiments were carried out according to the light industry standard of the People's Republic of China QB/T 2592-2003 Itaconic acid.

The residual amount of itaconic acid (bromine value) is calculated as mass fraction X, the value is expressed as %, according to formula (2):

$$X = \frac{(V_1 - V_2)/1000 \times c \times 65.05}{m} \times 100\% = \frac{(V_1 - V_2) \times c \times 0.06505}{m} \times 100\% \quad (2)$$

where: V_1 – the volume of $Na_2S_2O_3$ standard titration solution consumed during the blank test, mL; V_2 – the volume of $Na_2S_2O_3$ standard titration solution consumed during the titration of the specimen, mL; 65.05 – a molar mass of itaconic acid, g mol^{-1}; m – a mass of the specimen, g; 0.06505 – with 1.00 L standard solution of sodium thiosulfate [$c(Na_2S_2O_3)$ =

1.000 mol L^{-1}] equivalent to the mass of itaconic acid expressed in grams.

The monomer conversion rate α is calculated according to eqn (3):

$$\alpha = \left[1 - \frac{X \times m_0}{(M_{Br} \times 100) \times (m_1/M_1 + m_2/M_2 + m_3/M_3)}\right] \times 100\% \quad (3)$$

where: X – the residual amount of itaconic acid (bromine value), mg g^{-1}; M_{Br} – a relative molecular mass of bromine; m_0 – the total mass of monomer, g; m_1, m_2, m_3 – are the masses of each monomer, g; M_1, M_2, M_3 – are the relative molecular masses of each monomer, respectively.

3. Results and discussion

3.1 Characterization of polymer structure

3.1.1 FTIR analysis of IA-AM-SSS. In Fig. 2d, 3201 cm^{-1} is the O–H absorption peak in the carboxyl group of the copolymer, 3433 cm^{-1} absorption peak is attributed to the telescopic vibration of the N–H bond of the nonconjugated amide group, 2939 cm^{-1} is the absorption peak of the telescopic vibration of the methylene group, 1663 cm^{-1} is the absorption peak of the telescopic vibration of the carbonyl group, 1364 cm^{-1} absorption peak is attributed to the C–N telescopic vibration absorption of the amide group peak, 1180 cm^{-1} is the C–H deformation vibration (in-plane) of benzene ring, 1123 cm^{-1} is the asymmetric absorption peak of S=O bond of sulfonic acid group, 1034 cm^{-1} is the symmetric absorption peak of S=O bond of sulfonic acid group, 1007 cm^{-1} is the stretching vibration peak of S–O bond, 617 cm^{-1} is the C–S stretching absorption vibration peak, 920.05–784.92 cm^{-1} is the fingerprint of aromatic ring region, 832 cm^{-1} is the C–H stretching vibration peak of the aromatic ring (out-of-plane), 1412 and 1450 cm^{-1} correspond to two C=C stretching vibration absorption peaks of the aromatic ring backbone. In addition, combined with the absorption peak signal without the C=C bond at 1620–1640 cm^{-1}, it can be known that the monomer copolymerization reaction occurred, which proves that the polymer scale inhibitor molecule contains carboxylic acid group, amide group, sulfonic acid group, and other expected functional groups, and verifies the scale inhibiting activity of polymer scale inhibitor.

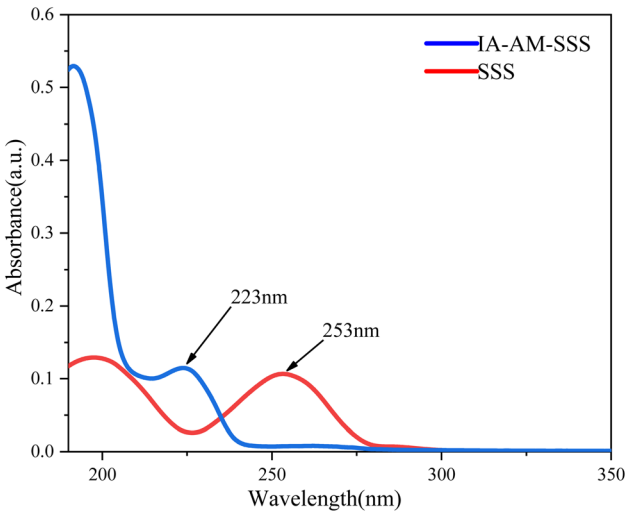

Fig. 3 UV spectra of IA-AM-SSS and SSS.

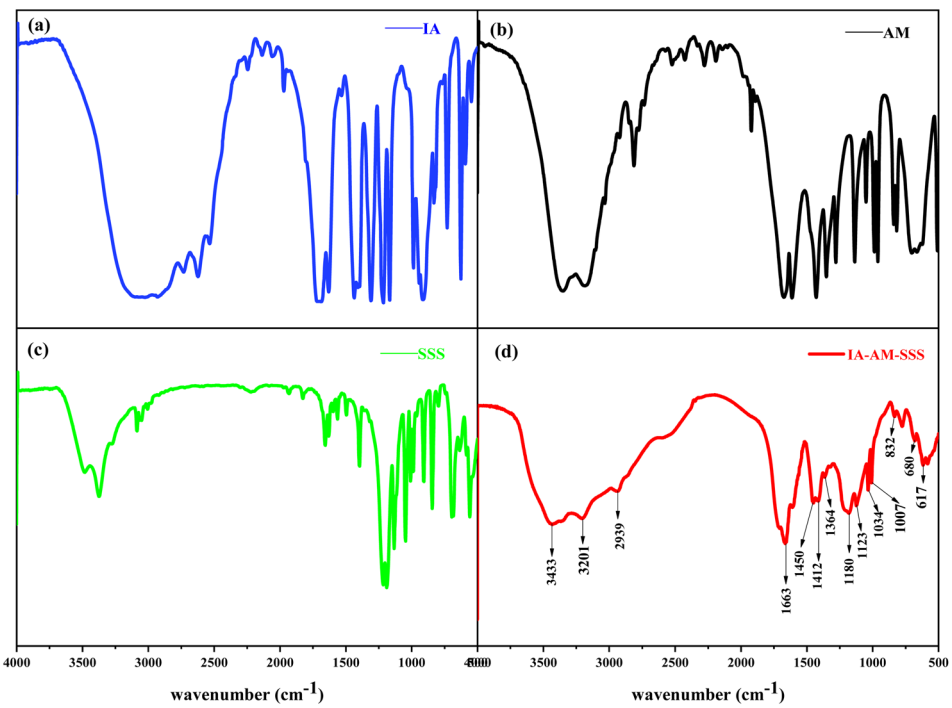

Fig. 2 The FTIR spectrum of (a) IA, (b) AM, (c) SSS, (d) IA-AM-SSS.

3.1.2 UV spectra of IA-AM-SSS polymer and SSS. The UV spectra of IA-AM-SSS and SSS (with water as solvent) are shown in Fig. 3. The characteristic peak of SSS appears at 253 nm in the B band (benzene-type band). It is the characteristic absorption band of aromatic compounds. It is an absorption band resulting from the vibration of the benzene ring itself and the $\pi \rightarrow \pi^*$ leap of the closed ring conjugated double bond, also known as the multiple absorptions of benzene. The maximum absorption peak of IA-AM-SSS copolymer is at 223.0 nm and is blue-shifted compared to the spectrum of SSS. This is mainly due to the electronic interactions between the chain groups and the aryl groups caused by the double bonds in the monomers acquired by the corresponding polymer chains through free radicals, resulting in a decrease in the ground state electronic energy level or an increase in the exciting state.[21,22]

3.1.3 ^{1}H-NMR spectra of IA-AM-SSS. The ^{1}H-NMR spectra of IA-AM-SSS are shown in Fig. 4. ^{1}H-NMR data are shown below, and the chemical and molecular structures were deduced as expected. ^{1}H NMR (400 MHz, D_2O), $\delta = 7.54$ (s, 2H), $\delta = 7.18$ (s, 2H), $\delta = 2.56$ (s, 3H), $\delta = 2.19$ (s, 7H), $\delta = 2.05$ (s, 7H), $\delta = 1.62$ (s, 7H), $\delta = 1.50$ (s, 10H). In combination with the above FTIR and UV analyses, the phosphorus-free polymer IA-AM-SSS was synthesized as expected.

3.2 Thermogravimetric analysis of copolymer

TG-DTG analysis is an important tool to assess the thermal stability of copolymers at different operating ambient temperatures, and the thermal weight loss curves of copolymers are shown in Fig. 5. At low heating rates, the degradation process leads to differential weight loss (DTG) curves with multiple peaks, which indicates the complexity of thermal degradation.[23,24] Thermal degradation from 0 to 100 °C is attributed to the evaporation of residual water and physically absorbed water. The mass loss of the copolymers, when heated to 130 °C, was about 10%, in addition to the maximum weight loss temperatures of 243 °C and 412 °C. The massive mass reduction was mainly due to the breakage of the side chain bonds of the copolymers and the thermal decomposition of groups such as carboxylic and sulfonic acid groups.[6] The residual mass of the copolymer at 800 °C was 16.64%, which could be attributed to the breakage of the C–C bond and benzene ring backbone in the molecule.[25] The above elucidates the thermal stability of the synthesized copolymers at different temperatures for rational application in oilfield water systems based on the test results.

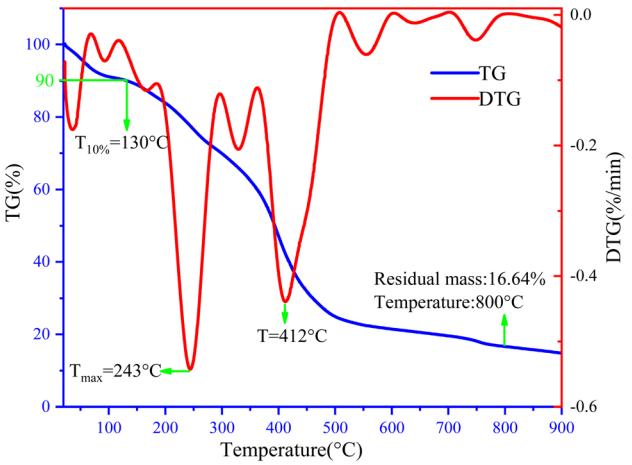

Fig. 5 Thermogravimetric analysis curve of IA-AM-SSS.

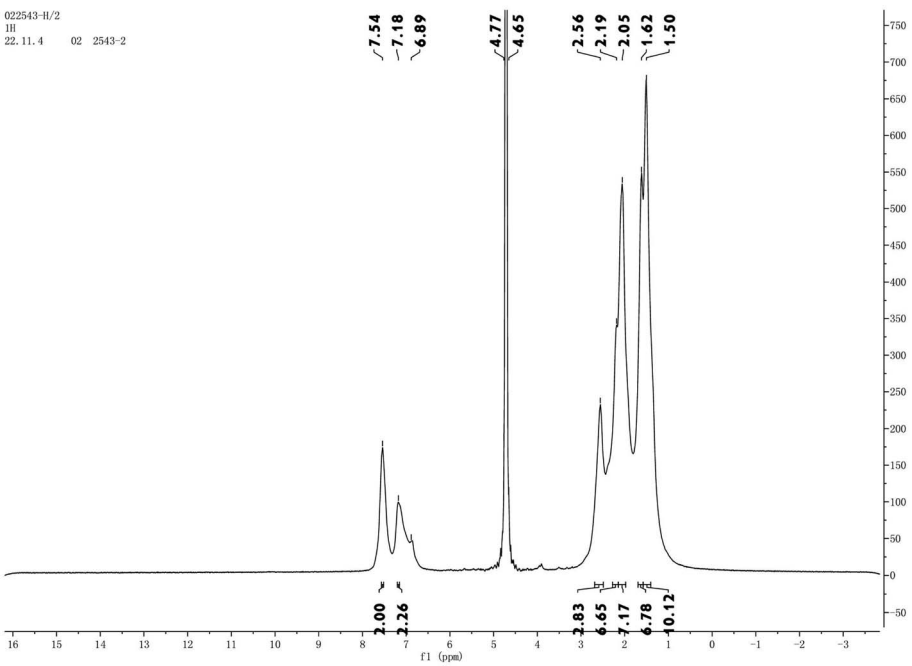

Fig. 4 ^{1}H NMR spectra of IA-AM-SSS and SSS.

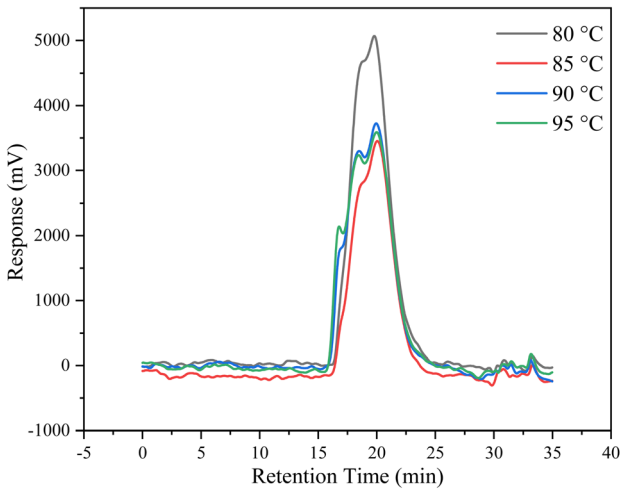

Fig. 6 GPC analysis of copolymers prepared at different temperatures.

3.3 Conversion rate and molecular weight distribution

The molecular weight distribution (MWD) of the synthesized copolymers was investigated using GPC at different temperatures, and the GPC curves of the synthesized copolymers are shown in Fig. 6. The GPC results for M_w, M_n, PDI (M_w/M_n), and conversion ratio results are shown in Table 1 (samples are noted as IAS). The PDI of the copolymer synthesized under the best conditions in the experiment was 3.67, which is a typical polymer dispersibility index in free radical polymerization, implying a suitably wide molecular weight distribution and polydispersity, and the proper polydispersity resulted in better thermal and aging resistance.[6,10,26] In addition, the molecular weight of the synthesized scale inhibitor is mostly in four orders of magnitude compared with the molecular weight of the monomer, which not only indicates the complete polymerization of the monomer but also can make use of the synergistic effect of various functional groups to make the copolymer have excellent scale inhibition properties.[6,15]

3.4 Optimum design of synthetic conditions of ter-copolymer

3.4.1 Effects of dosage and monomer ratio. The copolymer structure consists of hydrophobic and hydrophilic groups, with carboxyl and sulfonic acid groups as hydrophilic groups and benzene rings and carbon chains as hydrophobic groups.[27] In polymerization, the molar ratio of monomers has a great influence on the proportion of hydrophilic to hydrophobic groups in the final product.[28] Based on the data in Fig. 7 obtained from static experiments, the performance of copolymers prepared at different molar ratios was summarized (reaction conditions: initiator dosage of 6%, dropwise addition of 1 h, holding time of 1 h, the temperature of 80 °C), and it was determined that the scale inhibitor concentration and molar ratio had a great influence on the scale inhibiting performance of copolymers. In the selection of monomer ratio, since weak anionic monomers are affected by the electrostatic repulsion of strong anionic sulfonic acid groups, acrylamide is a water-soluble nonionic monomer and the reactivity is not affected by strong anionic groups.[8] So the fixed acrylamide dosage discusses the effect of the ratio of itaconic acid and sodium styrene sulfonate in the copolymer on its performance.

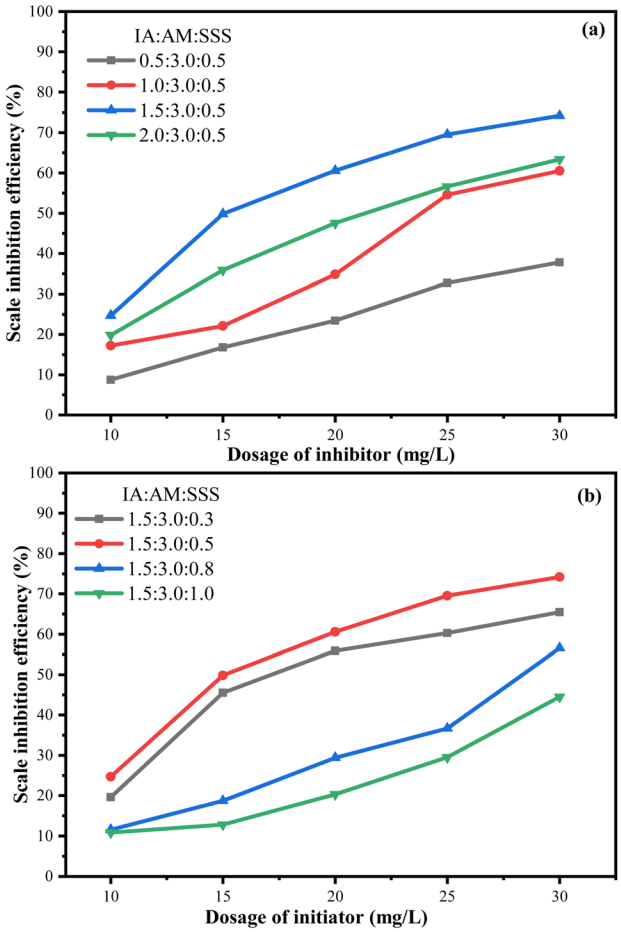

Fig. 7 Effect of dose and monomer ratio, (a) IA as variable, (b) SSS as variable.

Table 1 Conversion rate and molecular weight distribution of copolymers

Sample	Polymerization temperature/°C	Conversion rate (%)	M_n (g mol^{-1})	M_w (g mol^{-1})	PDI
IAS-80	80	96.3	25 941	95 329	3.67
IAS-85	85	98.1	24 123	90 099	3.73
IAS-90	90	95.9	28 391	135 453	4.77
IAS-95	95	95.3	27 834	158 679	5.70

As can be seen from Fig. 7a, when the monomer ratio of AM : SSS is $n(3.0):n(0.5)$, the inhibition efficiency of $CaCO_3$ starts to increase with the increase of the proportion of IA monomer in the copolymer, and the highest scale inhibition efficiency reaches 74.2%. The reason is that on the one hand, the hydrophilic group –COOH in IA is the main group to inhibit $CaCO_3$, and on the other hand, $–CONH_2$ in AM acts synergistically with the hydrophilic group –COOH to chelate with Ca^{2+} to achieve scale inhibition.[14,21,27,29] However, if the ratio of IA(–COOH) is too high, it is easy to form intramolecular hydrogen bonds in the copolymer and the hydrophilic chains are too long and entangled in flocculation, leading to a decrease in the inhibition efficiency of $CaCO_3$.[30]

Fig. 7b shows that the inhibition of the $CaCO_3$ scale by copolymers shows a trend of increasing and then decreasing with the increase of SSS monomer content, which is because the sulfonic acid group provided by SSS can improve the solubility of the product and stretch the free radical chain, thus improving the scale inhibition efficiency.[8,31] The strong charge density in the strongly hydrophilic $–SO_3H$ group makes SSS have favorable adsorption and complexation properties, which can effectively promote the complexation of copolymer with Ca^{2+} in water and thus inhibit the formation of $CaCO_3$.[4] However, when the proportion of SSS monomer was excessive, the scale inhibition efficiency decreased to 44.5%, which may be due to the ease of self-polymerization of excessive SSS, resulting in the decrease of scale inhibition efficiency of the copolymer.[28] The experimental results showed that when the monomer ratio of IA-AM-SSS was $n(\text{IA}):n(\text{AM}):n(\text{SSS}) = 1.5:3.0:0.5$, it had a good inhibition effect on $CaCO_3$.

3.4.2 Effect of dose and initiator dosage. In this work, the successful preparation of copolymers is inseparable from the decomposition and radical polymerization of the initiator. The amount of initiator in the reaction system determines the number of free radicals. Free radicals react with monomer molecules to form chain free radicals during the chain growth process. Different chain groups are finally terminated by double-radical coupling or double-radical disproportionation to synthesize polymers.[9] The rate and amount of free radical formation can affect the molecular weight of the polymer and lead to variations in the inhibitory effect. As can be seen from eqn (4), the kinetic chain length is inversely proportional to the square root of the initiator dose. (where, θ expresses kinetic chain length, and I is the amount of initiator)

$$\theta = \frac{k_p}{2(fk_dk_t)^{1/2}} \times \frac{M}{I^{1/2}} \quad (4)$$

The effect of initiator dosage and titration time on the scale inhibition performance was obtained by controlling the reaction conditions (monomer ratio $n(\text{IA}):n(\text{AM}):n(\text{SSS}) = 1.5:3.0:0.5$, holding time 1 h, temperature 80 °C). As shown in Fig. 8, when the initiating dose was lower than 8%, it was not enough to produce free radicals to react with the monomer.[2,28] If the amount of initiator is too small, the molecular chain of the polymeric scale inhibitor may become longer, and the molecular weight is too large, the functional groups on the molecular chain will increase relatively. If the functional groups reach a certain density, "flocculation" will occur, and calcium carbonate microcrystals will be wrapped and precipitated.[2] When the amount of initiator is greater than 8%, more free radicals are generated, which may lead to the synthesis of scale inhibitors with shorter molecular chains and smaller molecular weights. The functional groups of the copolymer cannot chelate the scale-forming ions well. And the negative charge density around the small molecular weight copolymer is low, which is not conducive to the repulsion between the particles. As a result, scale inhibition efficiency decreases slowly.[6,32] In addition, the polymerization reaction is smooth and orderly with good scale inhibition performance by appropriately extending the drop addition time.[28]

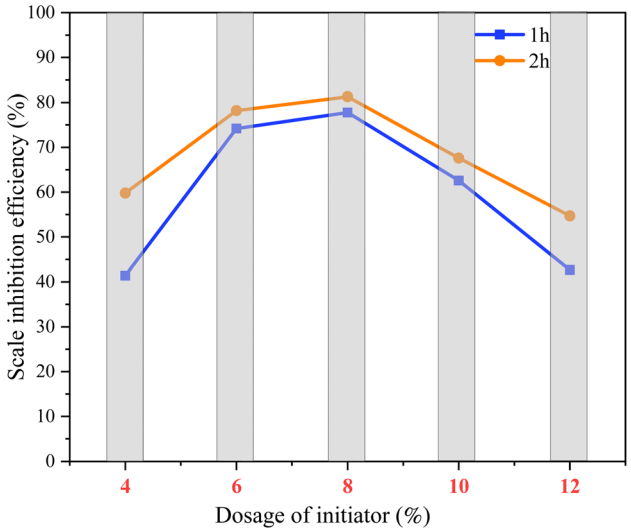

Fig. 8 Effects of initiator dose and drip time.

3.4.3 Effect of reaction temperature. A series of copolymer scale inhibitors with different molecular weights were prepared at different temperatures (reaction conditions: monomer ratio $n(\text{IA}):n(\text{AM}):n(\text{SSS}) = 1.5:3.0:0.5$, initiator dosage 8%,

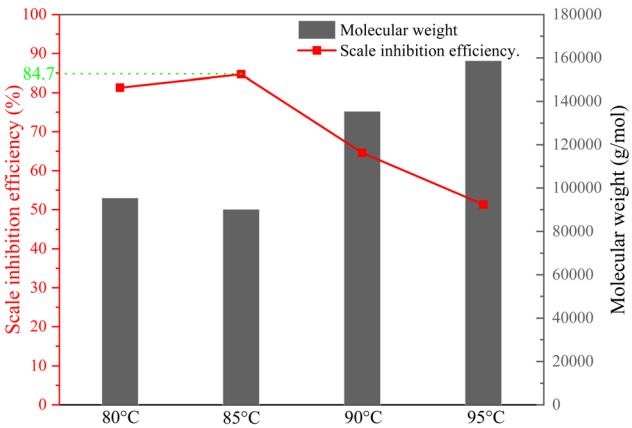

Fig. 9 Effect of temperature and molecular weight.

titration for 2 h and holding for 1 h), and the effect of reaction temperature on scale inhibition performance was obtained. The results are shown in Fig. 9. The scale inhibition of copolymer increased from 81.3% to 84.7% initially with the increase in temperature, and the scale inhibition decreased abruptly after rising to 90 °C. There are two possible reasons for this result.

The synthesis temperature affects the polymerization process by affecting the rate of decomposition of the initiator and the rate of molecular motion. The decomposition of the initiator is an endothermic reaction, and the lower reaction temperature hinders the decomposition of the initiator.[6] Therefore, the reduced scale inhibition efficiency of copolymers can be attributed to the presence of unreacted monomers and low polymerization. Table 1 if the temperature is too high, as the radical polymerization reaction is exothermic, higher temperatures decompose the radicals sufficiently, but the addition reaction between the primary radical and the monomer will be limited.[9]

$$k' = A'e^{-E/RT} \quad (5)$$

In addition, the scale inhibition performance of copolymers is closely related to the molecular weight, which determines the type of functional groups in the polymer.[12] The molecular weight of the products tends to decrease when the reaction temperature is increased from 80 to 85 °C. This phenomenon can be explained by eqn (5) (the formula for the integrated constant of polymerization), where the increase of reaction temperature leads to the increase of polymerization rate, and the molecular weight of the product gradually decreases. Therefore, the increase in scale inhibition efficiency may be due to the decrease in molecular weight, the high mobility of copolymer molecules, and the increased chance of collision between negatively charged functional groups and positively charged Ca^{2+}, which enhances the inhibitory effect of copolymer on calcium carbonate.[33] However, when the reaction temperature exceeds 90 °C, the increase in temperature leads to an increase in the polymerization rate and an excessive increase in the movement of molecular chains. As a result, the molecular weight of the product increases sharply, bridging and flocculation will play a leading role, so that the calcium scale will agglomerate and precipitate, and the scale inhibition rate of the copolymer will decrease.[25]

3.5 Morphology and physical phase analysis of calcium scale crystals

3.5.1 SEM of calcium carbonate crystal. SEM images of $CaCO_3$ obtained by adding different doses of copolymer scale inhibitor collection were obtained to reveal the potential mechanism of scale disruption by macromolecular scale inhibitors. This is shown in Fig. 10. In the absence of copolymer (Fig. 10a), $CaCO_3$ exhibited dense regular and uniform particle size with an overall symmetric monoclinic hexahedral morphology corresponding to the calcite phase.[19,34,35] When copolymer 10 mg L^{-1} was present in the test solution (Fig. 10b),

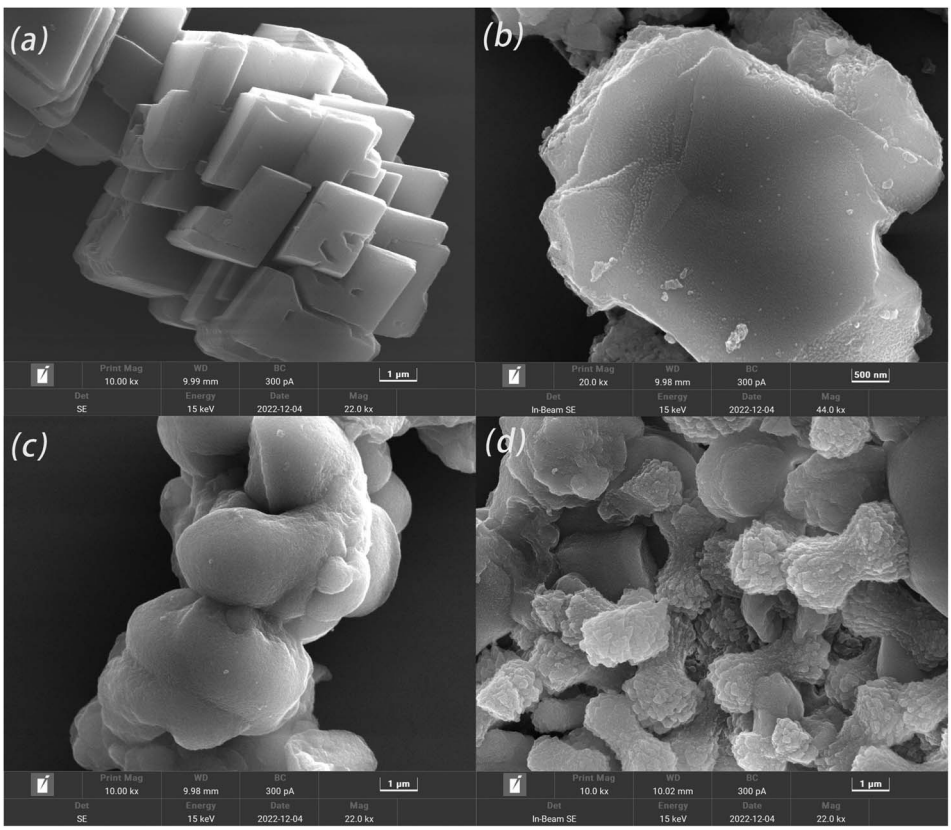

Fig. 10 SEM images for the calcium carbonate (a), with the presence of 10 mg L^{-1} (b), 20 mg L^{-1} (c), and 30 mg L^{-1} (d) IA-AM-SSS.

the structure of $CaCO_3$ deposits tended to break down, the rhombic sharp edges started to disappear and $CaCO_3$ lost its unbridged structure.[36] With the addition of copolymer 20 mg L^{-1} to the solution, the shape of $CaCO_3$ changed to a smooth grape-like ellipsoidal structure (Fig. 10c), and aragonite and vaterite replaced calcite to form thermodynamically unstable units.[37–39] With the addition of copolymers to the solution up to 30 mg L^{-1}, loose crystals of dumbbell and spherical shapes with very small particle sizes were obtained (Fig. 10d). These aggregates were easily dispersed and had poor adhesion to the cup wall. In conclusion, the SEM results indicate that the copolymer adsorbs on the crystal surface and disturbs the regular growth of $CaCO_3$ crystals leading to a distortion of the scale, which leads to a change in the crystal morphology of the precipitation.

3.5.2 FTIR analysis of $CaCO_3$ crystal. Fig. 11 shows the FTIR spectra of $CaCO_3$ crystals, which tentatively confirms the crystallographic variation of $CaCO_3$ crystals. The $CaCO_3$ crystals obtained in control (Fig. 11a) are mainly calcite, and the peaks at 711 cm^{-1}, 1413 cm^{-1}, and 1799 cm^{-1} are the characteristic absorption peaks of $CaCO_3$ crystalline calcite. In Fig. 11b after the addition of a copolymer scale inhibitor, the peaks at 745 cm^{-1}, and 1455 cm^{-1} are absorption from $CaCO_3$ crystalline vaterite.[39,40] It indicates that the added copolymer scale inhibitor converts the $CaCO_3$ crystals from calcite to vaterite, which helps to dissolve the scale.

3.5.3 XRD analysis of $CaCO_3$ crystal. In addition to the use of FTIR analysis, the $CaCO_3$ crystals were further subjected to physical phase analysis by XRD to identify the crystalline phases and further investigate the scale inhibition mechanism. Fig. 12 shows the XRD spectra of $CaCO_3$ crystals prepared in the presence and absence of copolymer. $CaCO_3$ crystals can contain several types of crystal forms, *i.e.* calcite, aragonite, and vaterite,

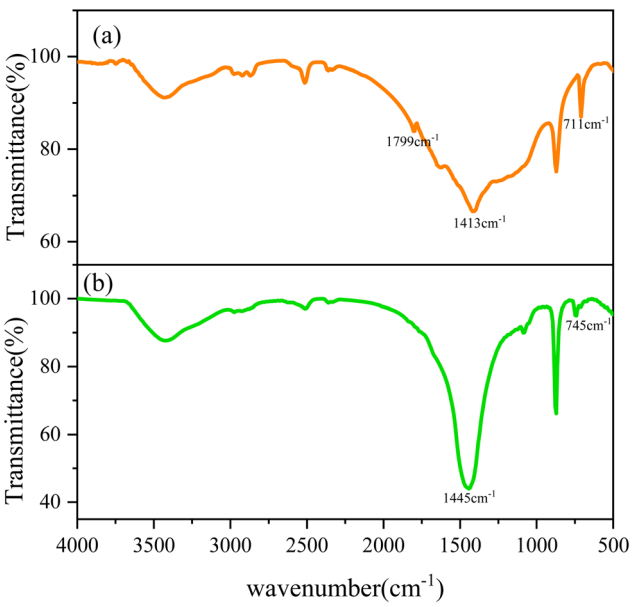

Fig. 11 FTIR spectra of $CaCO_3$ without IA-AM-SSS (a) and with IA-AM-SSS (b).

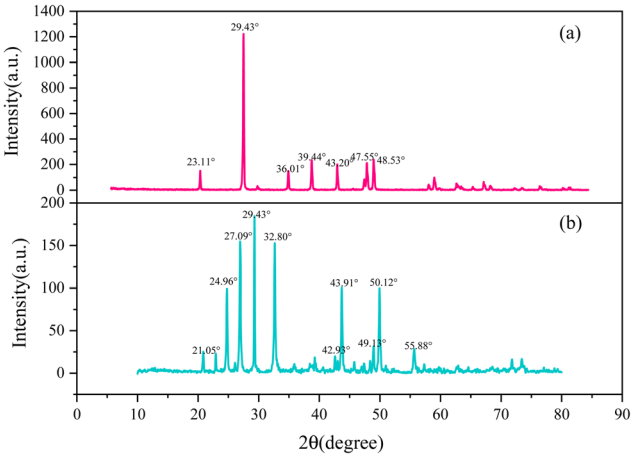

Fig. 12 XRD spectra of $CaCO_3$ without IA-AM-SSS (a) and with IA-AM-SSS (b).

where calcite is the most thermodynamically stable form, and the crystal forms usually contain multiple characteristic diffraction peaks with different characteristic diffraction peaks corresponding to different diffraction angles (2θ).[38] In Fig. 12a, the diffraction peaks at 23.12°, 29.43°, 36.01°, 39.44°, 43.2°, 47.55° and 48.53° correspond to stable calcite crystals (PDF = 47–1743), indicating that the structure of the blank control $CaCO_3$ crystals is mainly calcite. In Fig. 12b, the peak at 42.93° corresponds to a sub-stable aragonite crystal (PDF = 41–1475), and the diffraction peaks at 21.05°, 24.96°, 27.09°, 32.80°, 43.91°, 49.13°, 50.12°, and 55.88° are all non-stationary spherical aragonite crystals (PDF = 33–0268).[10,19] It indicates that the copolymer scale inhibitor causes $CaCO_3$ to form mixed crystals, and the crystal form of $CaCO_3$ shows a tendency to change from calcite to vaterite.[11,41]

3.6 Discussion of scale inhibiting mechanisms

Based on the above results a possible inhibition mechanism is proposed as shown in Fig. 13. From a mechanistic point of view, the complexation effect, and crystal distortion all depend on the adsorption of the anionic charge inhibitor on the developing nucleus surface and the positively charged growth sites of the growing crystals.[27] IA-AM-SSS is a structurally well-defined triblock copolymer with negatively charged hydrophilic blocks of carboxylic acid groups, amide groups, and sulfonic acid groups on the side chains. The polymeric scale inhibitor is physically and chemically adsorbed on the calcium carbonate nucleus during the crystalline embryonic stage, making the nucleus particles negatively charged, and they form a double electric layer with the counter ions near the charged surface.[17] Due to electrostatic repulsion, which distorts the crystals and creates a laminar or porous structure, the crystals have difficulty aggregating to form a precipitate.[42] In this process, the carboxyl groups in the copolymer matrix recognize and encapsulate or form water-soluble complexes with positively charged calcium ions in solution or on the surface of inorganic minerals, which interfere and slow down crystal growth due to possible

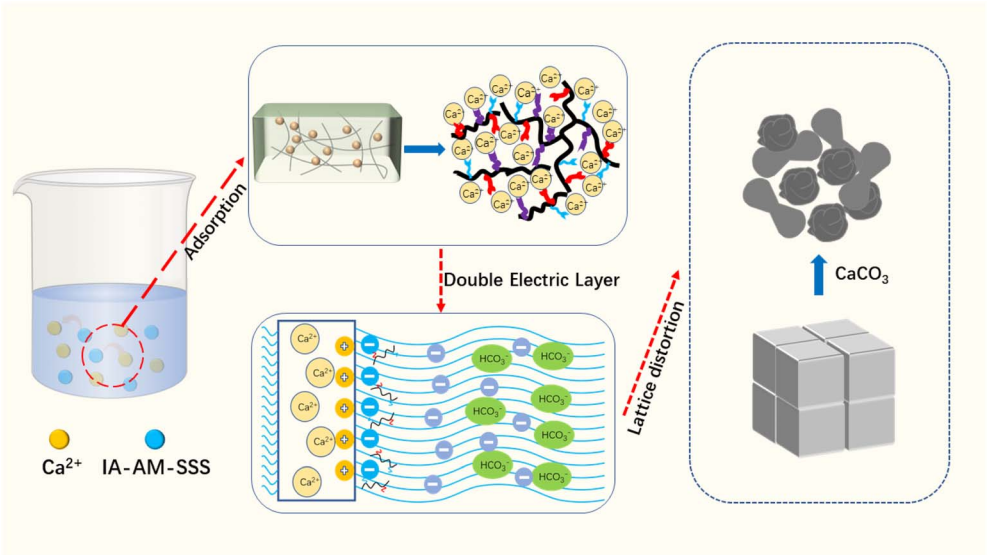

Fig. 13 Schematic of the scale inhibition mechanism of IA-AM-SSS.

adsorption at the active site of the nucleus.[38,43,44] Meanwhile, the N atoms of the lone pair and electronegative acrylamide not only chelate Ca^{2+} to delay scale formation, but also the arc-pair electrons can occupy the active site of calcium scale growth and reduce the rate of step movement across the crystal surface to prevent crystal growth.[19,29] In addition, the introduced sulfonic acid group exhibits strong hydrophilicity, which improves the water solubility and dispersibility of the scale inhibitor, which in turn improves the extension of the molecular chain, which encapsulates the crystal nuclei more easily and stably.[45]

4. Conclusions

A novel green phosphorus-free copolymer scale inhibitor was synthesized for the inhibition of calcium carbonate precipitation. It is considered a potential new environmentally safe water treatment agent for oilfield water systems. The main conclusions are as follows:

1. The copolymer has excellent scale inhibition performance under the following reaction conditions: $n(IA) : n(AM) : n(SSS) = 1.5 : 3.0 : 0.5$; ammonium persulfate is the total mass of the monomer 8% of (dropping 2 h); the reaction temperature is 85 °C, and the reaction time is 1 h. When the dosage is 30 mg L^{-1}, the scale inhibition rate can reach up to 84.7%, and the conversion rate is 98.1%.

2. IA-AM-SSS was identified as having the expected structure using FTIR, UV, and ^{1}H-NMR. TG-DTG showed that the synthesized copolymers had excellent thermal stability, with maximum mass loss temperatures of 243 °C and 412 °C for the copolymers and a residual mass ratio of 16.64% at 800 °C.

3. The scale inhibition performance of copolymers was influenced by their molecular weight, and the relative molecular mass distribution of copolymers was determined by using GPC. The GPC experiments demonstrated the effect law of different reaction temperatures on the molecular weight of copolymers, and the different reaction temperatures of copolymers directly led to the over or under the molecular weight of copolymers, which determined the inhibition performance of the $CaCO_3$ scale.

4. The analysis of crystals by SEM, FTIR, and XRD showed that the crystalline form and structure of calcium carbonate changed. In the absence of an inhibitor, $CaCO_3$ crystallized as rhombic calcite crystals, while in the presence of a copolymer, it was found to become a mixture of aragonite and vaterite crystals. The mechanism of inhibition of $CaCO_3$ based on these analyses hypothesized that a strong specific interaction of complexation and adsorption between the functional groups and the crystal surface occurs.

Conflicts of interest

There are no conflicts to declare.

References

1 M. F. Mady and M. A. Kelland, Study on Various Readily Available Proteins as New Green Scale Inhibitors for Oilfield Scale Control, *Energy Fuels*, 2017, **31**(6), 5940–5947, DOI: 10.1021/acs.energyfuels.7b00508.

2 X. Liu, X. Sheng, Q. Yao, L. Zhao, Z. Xu and Y. Zhou, Synthesis of a New Type of 2-Phosphonobutane-1,2,4-Tricarboxylic-Acid-Modified Terpolymer Scale Inhibitor and Its Application in the Oil Field, *Energy Fuels*, 2021, **35**(7), 6136–6143, DOI: 10.1021/acs.energyfuels.1c00167.

3 Y. Bu, Y. Zhou, Q. Yao, Y. Chen, W. Sun and W. Wu, Preparation and Evaluation of Nonphosphate Terpolymer as Scale Inhibitor and Dispersant for $Ca_3(PO_4)_2$, $BaSO_4$, and Iron (III) Hydroxide Scales, *J. Appl. Polym. Sci.*, 2015, **132**(9), DOI: 10.1002/app.41546.

4 Y. Chen, Y. Zhou, Q. Yao, Y. Bu, H. Wang, W. Wu and W. Sun, Preparation of a Low-Phosphorous Terpolymer as a Scale, Corrosion Inhibitor, and Dispersant for Ferric Oxide, *J. Appl. Polym. Sci.*, 2015, **132**(6), DOI: 10.1002/app.41447.

5 F. Jones, A. Oliveira, A. L. Rohl, G. M. Parkinson, M. I. Ogden and M. M. Reyhani, Investigation into the Effect of Phosphonate Inhibitors on Barium Sulfate Precipitation, *J. Cryst. Growth*, 2002, **237–239**, 424–429, DOI: 10.1016/S0022-0248(01)01961-3.

6 C. Cui and S. Zhang, Preparation, Characterization and Performance Evaluation of a Novel Scale Inhibiting and Dispersing Copolymer Containing Natural Tannin, *J. Polym. Environ.*, 2020, **28**(7), 1869–1879, DOI: 10.1007/s10924-020-01730-x.

7 C. Wang, D. Zhu and X. Wang, Low-Phosphorus Maleic Acid and Sodium ρ-Styrenesulfonate Copolymer as Calcium Carbonate Scale Inhibitor: Calcium Carbonate Scale Inhibitor, *J. Appl. Polym. Sci.*, 2010, **115**(4), 2149–2155, DOI: 10.1002/app.31300.

8 C. Cui and S. Zhang, Synthesis, Characterization and Performance Evaluation of an Environmentally Benign Scale Inhibitor IA/AMPS Co-Polymer, *New J. Chem.*, 2019, **43**(24), 9472–9482, DOI: 10.1039/C9NJ01355E.

9 H. Li, D. Ren, M. Zhuang, Z. Wang, X. Zhang, S. Zhang and W. Chen, Synthesis and Property Study of a Polyether Tercopolymer Scale Inhibitor with Carboxyl and Sulfonic Acid Groups, *J. Appl. Polym. Sci.*, 2022, **139**(3), 51505, DOI: 10.1002/app.51505.

10 X. Guo, X. Zhao, Y. Xu, P. Zhang, Y. Cheng and Y. Xu, The Synthesis of Polyaspartic Acid Derivative PASP-Im and Investigation of Its Scale Inhibition Performance and Mechanism in Industrial Circulating Water, *RSC Adv.*, 2020, **10**(55), 33595–33601, DOI: 10.1039/D0RA06592G.

11 S. Shi, X. Zhao, Q. Wang, H. Shan and Y. Xu, Synthesis and Evaluation of Polyaspartic Acid/Furfurylamine Graft Copolymer as Scale and Corrosion Inhibitor, *RSC Adv.*, 2016, **6**(104), 102406–102412, DOI: 10.1039/C6RA22048G.

12 L. Yang, W. Yang, B. Xu, X. Yin, Y. Chen, Y. Liu, Y. Ji and Y. Huan, Synthesis and Scale Inhibition Performance of a Novel Environmental Friendly and Hydrophilic Terpolymer Inhibitor, *Desalination*, 2017, **416**, 166–174, DOI: 10.1016/j.desal.2017.05.010.

13 L. Wang, C. Zhu, H. Liu, W. Zhao, Y. Che, Q. Zhang and L. Wang, Evaluation of Maleic Acid-based Copolymers Containing Polyoxyethylene Ether as Inhibitors for $CaCO_3$ Scale, *J. Appl. Polym. Sci.*, 2019, **136**(19), 47470, DOI: 10.1002/app.47470.

14 Y. Zuo, W. Yang, K. Zhang, Y. Chen, X. Yin and Y. Liu, Experimental and Theoretical Studies of Carboxylic Polymers with Low Molecular Weight as Inhibitors for Calcium Carbonate Scale, *Crystals*, 2020, **10**(5), 406, DOI: 10.3390/cryst10050406.

15 K. Cui, C. Li, B. Yao, F. Yang and G. Sun, Synthesis and Evaluation of an Environment-friendly Terpolymer $CaCO_3$ Scale Inhibitor for Oilfield Produced Water with Better Salt and Temperature Resistance, *J. Appl. Polym. Sci.*, 2020, **137**(11), 48460, DOI: 10.1002/app.48460.

16 Y. Liu, Y. Zhou, Q. Yao, H. Wang, Z. Wu, Y. Chen, L. Liu, C. Yang, W. Wu and W. Sun, Preparation of a Multifunctional Terpolymer Inhibitor for $CaCO_3$ and $BaSO_4$ in Oil Fields, *Tenside, Surfactants, Deterg.*, 2016, **53**(2), 148–156, DOI: 10.3139/113.110420.

17 Y. Xu, L. Zhao, L. Wang, S. Xu and Y. Cui, Synthesis of Polyaspartic Acid–Melamine Grafted Copolymer and Evaluation of Its Scale Inhibition Performance and Dispersion Capacity for Ferric Oxide, *Desalination*, 2012, **286**, 285–289, DOI: 10.1016/j.desal.2011.11.036.

18 B. Zhang, D. Zhou, X. Lv, Y. Xu and Y. Cui, Synthesis of Polyaspartic Acid/3-Amino-1H-1,2,4-Triazole-5-Carboxylic Acid Hydrate Graft Copolymer and Evaluation of Its Corrosion Inhibition and Scale Inhibition Performance, *Desalination*, 2013, **327**, 32–38, DOI: 10.1016/j.desal.2013.08.005.

19 S. Shi, D. Li, C. Chai, Y. Wu and Y. Xu, Synthesis of a Polyaspartic Acid/4-(2-Aminoethyl) Morpholine Graft Copolymer and Evaluation of Its Scale and Corrosion Inhibition Performance, *Polym. Adv. Technol.*, 2018, **29**(11), 2838–2847, DOI: 10.1002/pat.4406.

20 H. Zhang, J. Zhuang, S. Huang, X. Cheng, Q. Hu, Q. Guo and J. Guo, Synthesis and Performance of Itaconic Acid/Acrylamide/Sodium Styrene Sulfonate as a Self-Adapting Retarder for Oil Well Cement, *RSC Adv.*, 2015, **5**(68), 55428–55437, DOI: 10.1039/C5RA05167C.

21 X. Gu, F. Qiu, X. Zhou, J. Qi, Y. Zhou, X. Guo and D. Yang, Preparation, Characterization, and Inhibition Efficiency of Quadripolymer for Use as Scale Inhibitor, *Int. J. Polym. Anal. Charact.*, 2012, **17**(5), 321–332, DOI: 10.1080/1023666X.2012.668451.

22 X. Gu, F. Qiu, X. Zhou, J. Qi, Y. Zhou, D. Yang, Q. Guo and X. Guo, Preparation and Application of Polymers as Inhibitors for Calcium Carbonate and Calcium Phosphate Scales, *Int. J. Polym. Mater. Polym. Biomater.*, 2013, **62**(6), 323–329, DOI: 10.1080/00914037.2012.670824.

23 X. Guo, F. Qiu, K. Dong, X. Zhou, J. Qi, Y. Zhou and D. Yang, Preparation, Characterization and Scale Performance of Scale Inhibitor Copolymer Modification with Chitosan, *J. Ind. Eng. Chem.*, 2012, **18**(6), 2177–2183, DOI: 10.1016/j.jiec.2012.06.015.

24 X. Ma, M. Zhang, M. Zhao and L. Yang, Synthesis of MA/AA/MA-β-CD/SHP Quadripolymer and Its Performance Evaluation as Scale Inhibitor, *Russ. J. Appl. Chem.*, 2018, **91**(8), 1322–1331, DOI: 10.1134/S1070427218080104.

25 M. Zhou, Y. Gu and R. Yi, Preparation and Performance Evaluation of a New Ter-Polymer Scale Inhibitor, *J. Macromol. Sci., Part A*, 2019, **56**(11), 1060–1070, DOI: 10.1080/10601325.2019.1652544.

26 C. Cui and S. Zhang, Synthesis, Scale Inhibition and Dispersion Performance Evaluation of the Environmentally Benign Additive IA–AMPS–APEG Copolymer, *Environ. Sci.: Water Res. Technol.*, 2019, **5**(10), 1736–1747, DOI: 10.1039/C9EW00506D.

27 K. K. Kommanapalli, P. Lyot, J. R. Sunkara, P. Cheucle, A. V. L. N. S. H. Hari Haran and P. Mulukutla, Synthesis and Characterization of Maleic Acid and Sodium Methallyl

Disulfonate New Copolymer: Application as a Barium Sulfate Scale Inhibitor, *J. Pet. Explor. Prod. Technol.*, 2019, **9**(1), 223–232, DOI: 10.1007/s13202-018-0450-7.

28 Y. Bao, M. Li and Y. Zhang, Research on the Synthesis and Scale Inhibition Performance of a New Terpolymer Scale Inhibitor, *Water Sci. Technol.*, 2016, **73**(7), 1619–1627, DOI: 10.2166/wst.2015.635.

29 Y. Zhang, H. Yin, Q. Zhang, Y. Li and P. Yao, Synthesis and Characterization of Novel Polyaspartic Acid/Urea Graft Copolymer with Acylamino Group and Its Scale Inhibition Performance, *Desalination*, 2016, **395**, 92–98, DOI: 10.1016/j.desal.2016.05.020.

30 J. Li, Y. Zhou, Q. Yao, T. Wang, A. Zhang, Y. Chen, W. Wu and W. Sun, Preparation and Evaluation of a Polyether-Based Polycarboxylate as a Kind of Inhibitor for Water Systems, *Ind. Eng. Chem. Res.*, 2017, **56**(10), 2624–2633, DOI: 10.1021/acs.iecr.6b04427.

31 G. Zhang, J. Ge, M. Sun, B. Pan, T. Mao and Z. Song, Investigation of Scale Inhibition Mechanisms Based on the Effect of Scale Inhibitor on Calcium Carbonate Crystal Forms, *Sci. China, Ser. B: Chem.*, 2007, **50**(1), 114–120, DOI: 10.1007/s11426-007-0010-3.

32 M. Zhou, Y. Gu, R. Yi and H. Han, Synthesis and Property Study of Ter-Copolymer P(MA-AMPS-HPA) Scale Inhibitor, *J. Polym. Res.*, 2020, **27**(10), 294, DOI: 10.1007/s10965-020-02270-7.

33 Y. Wang, A. Li and H. Yang, Effects of Substitution Degree and Molecular Weight of Carboxymethyl Starch on Its Scale Inhibition, *Desalination*, 2017, **408**, 60–69, DOI: 10.1016/j.desal.2017.01.006.

34 H. Luo, D. Chen, X. Yang, X. Zhao, H. Feng, M. Li and J. Wang, Synthesis and Performance of a Polymeric Scale Inhibitor for Oilfield Application, *J. Pet. Explor. Prod. Technol.*, 2015, **5**(2), 177–187, DOI: 10.1007/s13202-014-0123-0.

35 H. Huang, Q. Yao, H. Chen and B. Liu, Scale Inhibitors with a Hyper-Branched Structure: Preparation, Characterization and Scale Inhibition Mechanism, *RSC Adv.*, 2016, **6**(95), 92943–92952, DOI: 10.1039/C6RA21091K.

36 Y. Liu, Y. Zhou, Q. Yao and W. Sun, Evaluating the Performance of PEG-Based Scale Inhibition and Dispersion Agent in Cooling Water Systems, *Desalin. Water Treat.*, 2015, **56**(5), 1309–1320, DOI: 10.1080/19443994.2014.944220.

37 Z. Shen, X. Zhi and P. Zhang, Preparation of Fluorescent Polyaspartic Acid and Evaluation of Its Scale Inhibition for $CaCO_3$ and $CaSO_4$: Preparation and Evaluation of Fluorescent Polyaspartic Acid, *Polym. Adv. Technol.*, 2017, **28**(3), 367–372, DOI: 10.1002/pat.3897.

38 W. Zhang, G. Li, F. Jin, Y. Huo, T. Sun and C. Li, Synthesis and Characterization of an Ionic Liquid–Carboxylic Acid Copolymer Scale Inhibitor and Its Scale Inhibition Performance, *Water Supply*, 2019, **19**(5), 1463–1472, DOI: 10.2166/ws.2019.011.

39 Z. Zhang, T. Liang, J. Liu, K. Ding and H. Chen, Hyperbranched Polyesters with Carboxylic Acid Functional Groups for the Inhibition of the Calcium Carbonate Scale, *J. Appl. Polym. Sci.*, 2018, **135**(23), 46292, DOI: 10.1002/app.46292.

40 G. Zhang, J. Ge, M. Sun, B. Pan, T. Mao and Z. Song, Investigation of Scale Inhibition Mechanisms Based on the Effect of Scale Inhibitor on Calcium Carbonate Crystal Forms, *Sci. China, Ser. B: Chem.*, 2007, **50**(1), 114–120, DOI: 10.1007/s11426-007-0010-3.

41 H. Huang, Q. Yao, Q. Jiao, B. Liu and H. Chen, Polyepoxysuccinic Acid with Hyper-Branched Structure as an Environmentally Friendly Scale Inhibitor and Its Scale Inhibition Mechanism, *J. Saudi Chem. Soc.*, 2019, **23**(1), 61–74, DOI: 10.1016/j.jscs.2018.04.003.

42 S. Kim, J. Kim, S. Kim, J. Lee and J. Yoon, Electrochemical Lithium Recovery and Organic Pollutant Removal from Industrial Wastewater of a Battery Recycling Plant, *Environ. Sci.: Water Res. Technol.*, 2018, **4**(2), 175–182, DOI: 10.1039/C7EW00454K.

43 F. Change, Z. Yuming, L. Guangqing, H. Jingyi, S. Wei and W. Wendao, Inhibition of $Ca_3(PO_4)_2$, $CaCO_3$, and $CaSO_4$ Precipitation for Industrial Recycling Water, *Ind. Eng. Chem. Res.*, 2011, **50**(18), 10393–10399, DOI: 10.1021/ie200051r.

44 Y. Wang, H. Chen, Z. Zhang, H. Huang, B. Liu and K. Ding, Synthesis and Characterization of PBTCA-modified Hyperbranched Polyether Corrosion and Scale Inhibitors, *J. Appl. Polym. Sci.*, 2019, **136**(38), 48041, DOI: 10.1002/app.48041.

45 G. Liu, M. Xue, J. Huang, H. Wang, Y. Zhou, Q. Yao, L. Ling, K. Cao, Y. Liu, Y. Bu, Y. Chen, W. Wu and W. Sun, Preparation and Application of a Phosphorous Free and Nonnitrogen Scale Inhibitor in Industrial Cooling Water Systems, *Front. Environ. Sci. Eng.*, 2015, **9**(3), 545–553, DOI: 10.1007/s11783-014-0657-x.